

# Stability Analysis of Heston Characteristic Function with Optimal Volatility Parameters

Kodwo Annan<sup>1</sup>, Alidu Salifu<sup>2</sup> and Daniel Ngugi<sup>3</sup>

## Abstract

Heston volatility model has received a growing attention amongst academics and practitioners for derivative pricing applications. Yet, the sensibility of the model parameters and instabilities of its analytic characteristic function for large derivatives and complex derivations make the model inconsistent and unreliable. As these parameters and function are defined and used in the complex plane, they potentially include ‘branching’. Therefore, additional parameter restrictions are required. This paper aims at providing insight on the sensitivity of the model parameterization and establishing an algorithm to ensure the stability of the analytic characteristic function under full dimensional and unrestricted parameter space.

**Keywords:** Heston Model, Characteristic Function, Stability Analysis, Stochastic Volatility, Parameter

---

<sup>1</sup> Minot State University (MSU), Math & Comp. Dept.

<sup>2</sup> MSU, Energy Economics & Finance Dept.

<sup>3</sup> MSU, Economics Department.

## 1 Introduction

The Black-Scholes model (BSM) developed by Fischer Black and Myron Scholes in 1973 [1] was revolutionary in its impact on the financial industry. Ever since the introduction of the model, academics and practitioners have made numerous attempts to relax the restrictive assumptions that make the model inconsistent with observed prices in the market. Particular interest has been directed towards the assumption of constant volatility, which makes the model unable to generate non-normal return distributions and the well-known volatility smile, consistent with empirical findings on asset returns [2].

Examples of extensions of BSM include models that allow for stochastic volatility in the underlying return process. When stochastic volatility is applied, it improves on the BSM assumption by making volatility dependent on additional parameters such as distribution of returns and variance itself. Many different stochastic volatility models have been proposed [3-11], but one that has received a growing attention amongst academics and practitioners for derivative pricing is the Heston Model [11].

Heston Model's attractiveness lies in the powerful duality of its tractability and robustness relative to other stochastic volatility models. The major advantages of the model include equity returns and implied volatility of the option prices, flexibility for non lognormal probability distributions, mean-reverting volatility and a closed form analytic characteristic function for fast calibration of option prices. While these parameters and analytic characteristic function have been well studied, their formulation and analysis have shown discontinuity/instability in the time domain which arises from the branch cut of the principle branch of logarithm.

Investigators [12-15] of the branches of the logarithm on Heston's characteristic function have suggested that the associated logarithm is continuous on the time domain whenever restrictive conditions are imposed on the model

---

parameters. However, for large enough maturities under certain parameters, instabilities are observed [15]. To perform well across large time interval of maturities, unrestricted parameter space is necessary to guarantee the stability of the model. Rather than imposing restrictive conditions on the Heston characteristic function, we show in this paper that continuity and stability of Heston's model is guaranteed under full dimensional and unrestricted parameter space.

The rest of the paper is structured as follows: In section 2, we formulate Heston stochastic volatility model for price option. We follow the model formulation by a sensibility analysis on the model's initial conditions and parameters in section 3. The analytic characteristic function generation and its stability analysis for unrestricted parameter space are established in section 4. Conclusion follows in section 5.

## 2 Model Formulation

Consider  $S = \{S_t : 0 < t < T\}$  as a stock price process and  $\Phi_T(\bullet)$  as the characteristic function of the nature logarithm of the terminal stock price  $s_T = \ln(S_T)$ . Let  $W_t$  denotes a Wiener process and the constants  $r$  and  $\delta$  representing, respectively, the continuous interest rate and dividend gained. Then, the stochastic volatility model underlying the dynamics of the spot price is given by Heston [11] as

$$\begin{aligned} \frac{dS_t}{S_t} &= (r - q)dt + \sigma_t dW_t^1, \\ dV_t &= \kappa(\theta - V_t)dt + \zeta\sigma_t dW_t^2, \\ \text{Cov}[dW_t^1, dW_t^2] &= \rho dt, S(t=0) = S_0, V(t=0) = V_0. \end{aligned} \quad (1)$$

As usual  $S_t$  denotes the spot at time  $t$ ,  $V_t$  is either the volatility (i.e. when  $\sigma_t = V_t$ ) of or the variance (i.e. when  $\sigma_t = \sqrt{V_t}$ ) of the underlying,  $r$  is the

risk-free rate of return,  $q$  is the dividend yield,  $\{W_t^1, W_t^2\}_{t \geq 0}$  representing the two Wiener processes with constant correlation coefficient  $\rho$  such that  $|\rho| < 1$ , and the parameters  $\kappa, \theta$  and  $\zeta$  denoting the rate of mean reversion, the long-run mean of the variance and the volatility of the variance process, respectively, are all nonnegative.

Since the process  $\{S_t\}_{t \geq 0}$  can be written as the exponential of a smooth functional of the variance process, it has a strong unique solution. The main property of a strong solution of  $\{S_t\}_{t \geq 0}$  is with respect to the filtration  $\{F_t\}_{t \geq 0}$ . This implies that heuristically the solution should be a measurable function of the initial condition and the Wiener process. However, since the square-root function is not smooth at the origin, understanding the behavior of the variance process at that point is vital.

Ideally one would like a variance process which is strictly positive, because otherwise it degenerates to a deterministic function for the time it stays at zero.

Feller condition, [16], given by  $\alpha = \frac{4\kappa\theta}{\zeta^2} \geq 2$  where  $\alpha$  is the dimensionality of

the corresponding Bessel process normally assures strictly positive variance process. Unfortunately, when calibrating the Heston model to market option prices it is not uncommon for the parameters to violate the Feller condition. It is also seen that model equation (1) is incomplete when comparing the number of random process (two Wiener process) with the number of the risky traded assets (only the underlying spot). Therefore, it is not possible to obtain a unique price for any contingent claim using only the underlying spot. That is why one has to add a European call, for example, when completing market with Heston Model.

### 3 Initial and Calibration Parameters

To reduce dimensionality problem, it is important to understand the initial parameter ( $V_0$ ) and calibration parameters ( $\kappa, \rho, \zeta$ ) under Heston model. Changing the initial variance,  $V_0$ , of the model allows adjustment in the height of the curve rather than the shape. Increasing the initial volatility level moved the implied volatility curve upwards, (see Figure 1a). However, increasing the volatility of variance  $\zeta$  has significant impact on the implied volatility. As shown in Figure 1b, increasing  $\zeta$  makes the smile more prominent in addition to creating heavy tails on both sides. This makes sense because higher volatility of variance means volatility is more volatile and so the market has a greater change of extreme movements. So, writers of puts must charge more and those of calls less, for a given strike. Also, this impact produces barrage of distributions which make the model more robust and therefore creates framework for option price variety.

The long-run mean  $\theta$  and  $V_0$  have similar influence upon the implied volatility curve (Figure 2a). It seems efficient to choose the initial variance a priori, e.g. setting the root of  $V_0$  as the implied at-the-money (ATM) volatility, and only allow  $\theta$  varying. In particular, a different initial variance for different maturities would be inconsistent for our model.

The mean reversion rate  $\kappa$  can be interpreted as the degree of volatility clustering, meaning large moves are followed by large moves while small moves are followed by small moves. The parameter  $\kappa$  controls the curvature of the curve. Increasing  $\kappa$  flattens the implied volatility smile, see Figure 2b. Decreasing the mean reversion has a similar effect as increasing the volatility of variance in terms of curvature. In addition, the high values of rate at which the variance process reverts to  $\theta$ , (that is  $\kappa$ ), essentially turn the stochastic volatility into a time dependent deterministic model. Moreover, the influence of  $\kappa$  is often compensated by a stronger  $\zeta$ . This suggests that can fix  $\kappa$  at some level, (say

1.5) and calibrate only the remaining three parameters. However, if the obtained parameters do not satisfy the Feller condition, then it might be worthwhile to fix higher  $\kappa$  and re-calibrating the other parameters to check if Feller condition is satisfied.

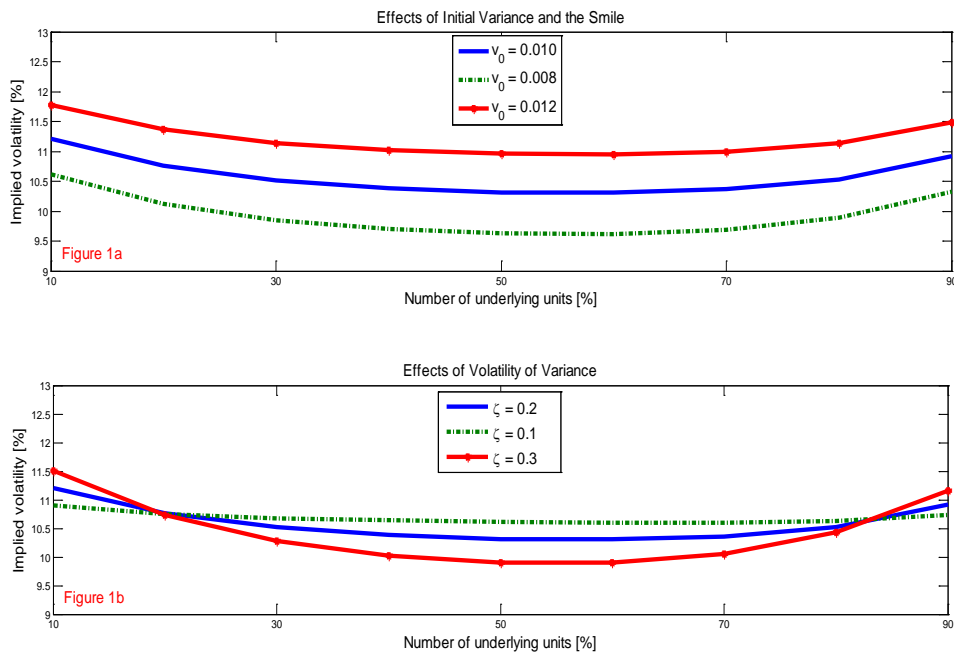


Figure 1: In Figure 1a, increasing the initial volatility  $V_0$  level moved the implied volatility curve upwards but did not affect the shape of the curve. However, increasing the volatility of variance  $\zeta$  affected the implied volatility curve significantly, as shown in Figure 1b. It creates heavy tails on both sides of the smile curve. This phenomenon provides a framework to price a variety of options that are close to reality. All smiles plotted in solid blue lines are obtained for  $V_0 = 0.01$ ,  $\kappa = 1.5$ ,  $\theta = 0.015$ ,  $\zeta = 0.2$  and  $\rho = 0.05$

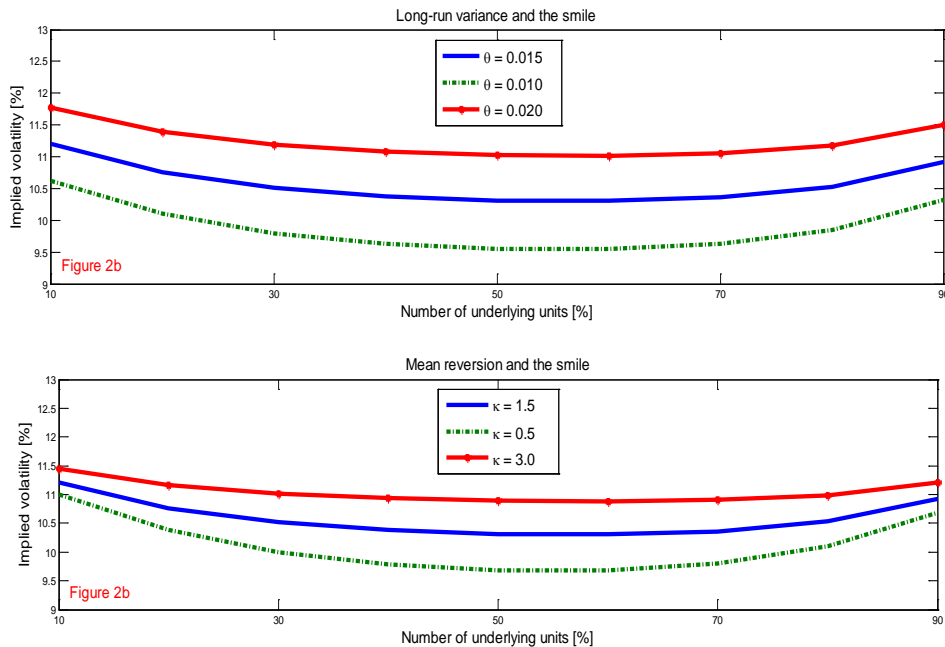


Figure 2: Figure 2a shows that the effect of the long-run mean  $\theta$  on the implied volatility smile curve is similar to the effect of initial variance on the smile curve. In Figure 2b, increasing the mean reversion parameter  $\kappa$  flattens the implied volatility smile and decreasing  $\kappa$  has a similar effect as increasing  $\zeta$  in terms of curvature.

The correlation  $\rho$ , which interprets the association between the log-returns and volatility of the asset, affects the implied volatility smile and the heaviness of the tails. Intuitively if  $\rho > 0$ , the volatility will increase as the asset price/return increases. Conversely, if  $\rho < 0$ , the volatility will increase when the asset price/return decreases. Uncorrelated case produces a smile curve that is not perfectly symmetric but centered at-the-money, see Figure 3a. Changing  $\rho$  changes the degree of symmetry. Thus, since lower returns are accompanied by higher volatility, negative  $\rho$  induces negative smile in the returns distribution. The reverse is true for positive correlation, Figure 3b.

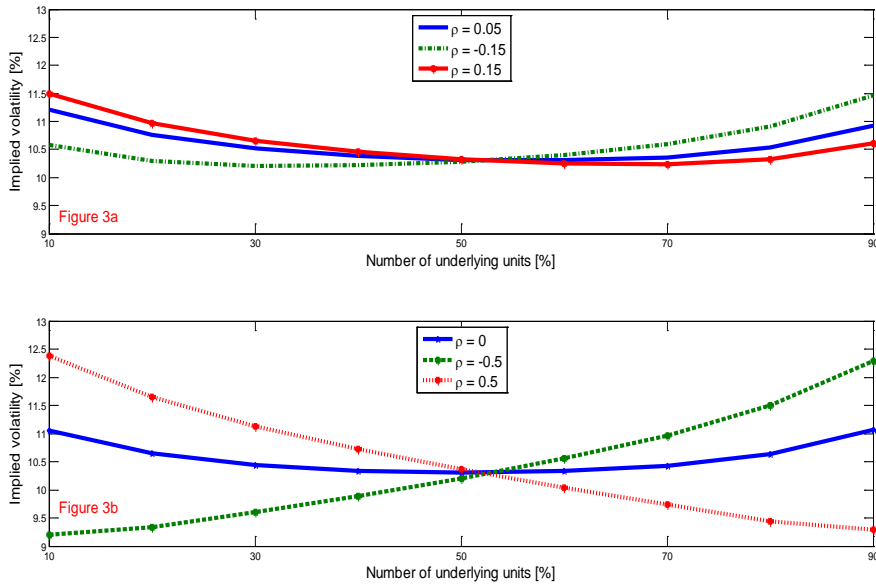


Figure 3: The effects of changing the correlation parameter  $\rho$  on the shape of the smile are given. For uncorrelated case, the smile curve is almost symmetric and centered, Figure 3b. Changing  $\rho$  changes the degree of symmetry. For positive correlation, volatility increases as the asset price/return increases. For negative correlation, volatility increases when asset price/return decreases. Varying  $\rho$  also impacts the shape of the implied volatility smile. Thus, the model can apply a variety of volatility smiles.

## 4 Stability of Heston Characteristic Function

There are three state variables in (1): the observed  $S_t$ , unobserved  $V_t$  and observed current time  $t \in [0, T]$ . Denoting the time to expiration by  $\tau = T - t$  and assuming that the process  $s_t = \ln(S_t)$  satisfies the stochastic differential equation (1), we closely follow Gatheral [17] to generate the characteristic function of  $s_T$

denoted by  $\Phi_T(\varphi)$  in the form

$$\Phi_T(\varphi) = S_0^{i\varphi} f(V_0, \varphi, T), \quad (2)$$

where  $i$  is the imaginary unit and

$$\begin{aligned} f(V_0, \varphi, T) &= \exp[A(\varphi, T) + B(\varphi, T)V_0], \\ A(\varphi, T) &= (r - q)Ti\varphi + \frac{\kappa\theta}{\sigma^2} \left[ (\kappa - i\varphi\rho\sigma - d)T - 2 \ln \left( \frac{1 - ge^{-dT}}{1 - g} \right) \right], \\ B(\varphi, T) &= \frac{\kappa - i\varphi\rho\sigma - d}{\sigma^2} \left[ \frac{1 - e^{-dT}}{1 - ge^{-dT}} \right], \\ d &= \sqrt{(\kappa - i\varphi\rho\sigma)^2 + \sigma^2(i\varphi + \varphi^2)}, \\ g &= (\kappa - i\varphi\rho\sigma - d)(\kappa - i\varphi\rho\sigma + d)^{-1}. \end{aligned} \quad (3)$$

We prove the necessary but sufficient stability condition of the characteristics function under the full dimensional and unrestricted parameter space.

Consider  $d(u) = \sqrt{(\kappa - i\varphi\rho\sigma)^2 + \sigma^2(i\varphi + \varphi^2)}$  given in (3), where now the dependence on  $\varphi$  is well-defined. At the negative real axis in the complex plane, we always have  $\text{Re}[d(\varphi)] > 0$ . In most Fast Fourier approaches for the calculation of option prices, the evaluation of the term  $\Phi_T[\varphi - (\alpha + 1)i]$  for  $\varphi > 0$  is necessary, where  $\alpha$  is a positive constant such that the  $(\alpha + 1)$ -th moment of the stock price exists. For simplicity, we denote  $\bar{d}(\varphi) = -d(\varphi - (\alpha + 1)i)$ . Implying

$$\bar{d}(\varphi) = -\sqrt{[\kappa - \rho\zeta\{\varphi - (\alpha + 1)i\}]^2 + \zeta^2\{\varphi - (\alpha + 1)i\}^2 + \zeta^2\{\varphi - (\alpha + 1)i\}^2}. \quad (4)$$

In order to avoid a discontinuity of  $\bar{d}(\varphi)$  at  $\varphi = 0$ , we choose  $\bar{d}(0) = \lim_{x \rightarrow 0} \bar{d}(\varphi)$  and so  $\varphi > 0$ .

**Theorem 4.1:** The function  $\bar{d}^*(\varphi) = d^*(\varphi - (\alpha + 1)i)$  does not cross the negative real axis as  $\varphi$  increases from zero to infinity.

**Proof:** Equation (4) can be expanded as

$$\bar{d}(\varphi) = -\sqrt{\zeta^2 \varphi^2 (1 - \rho^2) + (\kappa - \rho \zeta (\alpha + 1)) - \zeta^2 (\alpha + 1) \alpha - \varphi i (\zeta^2 (2\alpha + 1) + 2\rho \zeta (\kappa - \rho \zeta (\alpha + 1)))}. \quad (5)$$

Defining  $\bar{d}^*(\varphi) = d^*(\varphi - (\alpha + 1)i)$ , we examine five cases with respect to the signs of the three quantities  $\kappa - \rho \zeta (\alpha + 1)$ ,  $\zeta^2 (2\alpha + 1) + 2\rho \zeta (\kappa - \rho \zeta (\alpha + 1))$  and  $\rho$  to prove that  $\bar{d}^*(\varphi)$  does not cross the negative real axis. For  $\rho \leq 0$ , we see that  $\kappa - \rho \zeta (\alpha + 1) \geq 0$  and so two cases are examined:

CASE 1:  $\rho \leq 0$  and  $\zeta^2 (2\alpha + 1) + 2\rho \zeta (\kappa - \rho \zeta (\alpha + 1)) \leq 0$ . Thus

$$\bar{d}^*(\varphi) = \left( \frac{\kappa - \rho \zeta (\alpha + 1) - \rho \zeta \varphi i}{-\bar{d}(\varphi)} + 1 \right) - \left( \frac{\kappa - \rho \zeta (\alpha + 1) - \rho \zeta \varphi i}{-\bar{d}(\varphi)} - 1 \right) e^{\bar{d}(\varphi)t}. \quad (6)$$

The real part of  $\frac{\kappa - \rho \zeta (\alpha + 1) - \rho \zeta \varphi i}{-\bar{d}(\varphi)} \geq 0$ , as  $\text{Re}[\bar{d}(\varphi)] < 0$  and  $\text{Im}[\bar{d}(\varphi)] < 0$ .

Therefore,

$$\left| \frac{\kappa - \rho \zeta (\alpha + 1) - \rho \zeta \varphi i}{-\bar{d}(\varphi)} + 1 \right| \geq \left| \frac{\kappa - \rho \zeta (\alpha + 1) - \rho \zeta \varphi i}{-\bar{d}(\varphi)} - 1 \right| e^{-\alpha},$$

Hence for  $\text{Re} \left( \frac{\kappa - \rho \zeta (\alpha + 1) - \rho \zeta \varphi i}{-\bar{d}(\varphi)} + 1 \right) > 0$ , only the positive real axis can be crossed.

CASE 2:  $\rho \leq 0$  and  $\zeta^2 (2\alpha + 1) + 2\rho \zeta (\kappa - \rho \zeta (\alpha + 1)) > 0$ .

In this case  $\text{Re}(\bar{d}^*(\varphi)) < 0$  and  $\text{Im}(\bar{d}^*(\varphi)) > 0$  holds. Also notice that the square root expression of (5) can be written in the form

$$\sqrt{\Upsilon + iZ} = \sqrt{\frac{\Upsilon + \sqrt{\Upsilon^2 + Z^2}}{2}} + i \text{sgn } Z \sqrt{\frac{-\Upsilon + \sqrt{\Upsilon^2 + Z^2}}{2}}.$$

Thus,

$$\bar{d}(\varphi) = - \left( \sqrt{\frac{\sqrt{(A\varphi^2 - C)^2 + B^2\varphi^2} - (C - A\varphi^2)}{2}} - i \sqrt{\frac{\sqrt{(A\varphi^2 - C)^2 + B^2\varphi^2} + (C - A\varphi^2)}{2}} \right),$$

where

$$\begin{aligned} A &= \zeta^2(1 - \rho^2) > 0, \\ B &= \zeta^2(2\alpha + 1) + 2\rho\zeta(\kappa - \rho\zeta(\alpha + 1)) > 0, \\ C &= \zeta^2(\alpha + 1)\alpha - (\kappa - \rho\zeta(\alpha + 1))^2. \end{aligned}$$

Therefore, we are left to show that

$$0 \leq \arg\left(\frac{\kappa - \zeta\rho(\alpha + 1) - \zeta\rho\varphi i}{-\bar{d}^*(\varphi)}\right) \leq \frac{\pi}{2} \tag{7}$$

Recall that the numerator of (7) lies in the first quadrant while the denominator lies in the fourth quadrant. Clearly, (7) is true when  $\rho = 0$ . For  $\rho < 0$  and  $\varphi = 0$ , equation(7) becomes

$$0 \leq \arg\left(\frac{\kappa - \zeta\rho(\alpha + 1) - \zeta\rho\varphi i}{-\bar{d}^*(\varphi)}\right) = \begin{cases} \frac{\pi}{2}; & C > 0 \\ 0; & C \leq 0. \end{cases} \tag{8}$$

For  $\varphi > 0$ , we have

$$\arg\left(-\bar{d}^{*-1}(\varphi)\right) = \tan^{-1}\left(\frac{\sqrt{\frac{\sqrt{(A\varphi^2 - C)^2 + B^2\varphi^2} + (C - A\varphi^2)}{2}}}{\sqrt{\frac{\sqrt{(A\varphi^2 - C)^2 + B^2\varphi^2} - (C - A\varphi^2)}{2}}}\right).$$

So, equation (7) becomes

$$0 \leq \tan^{-1}\left(\frac{C - A\varphi^2 + \sqrt{B^2\varphi^2 + (C - A\varphi^2)^2}}{B\varphi}\right) \leq \frac{\pi}{2} - \tan^{-1}\left(\frac{-\zeta\rho\varphi}{\kappa - \zeta\rho(\alpha + 1)}\right) \leq \frac{\pi}{2}, \tag{9}$$

which lies between zero and  $\pi/2$ . Thus, applying  $\tan(\cdot)$  to both sides of (9) we have

$$\begin{aligned} \frac{C - A\varphi^2 + \sqrt{B^2\varphi^2 + (C - A\varphi^2)^2}}{B\varphi} &\leq \frac{\kappa - \zeta\rho(\alpha + 1)}{-\zeta\rho\varphi}, \\ \Rightarrow B(\kappa - \rho\zeta(\alpha + 1)) + C\zeta\rho - A\zeta\rho\varphi^2 &\geq -\zeta\rho\sqrt{B^2\varphi^2 + (C - A\varphi^2)^2}. \end{aligned} \tag{10}$$

Both sides of (10) are positive since the right hand side is obvious and the left hand side is

$$\begin{aligned} B(\kappa - \rho\zeta(\alpha + 1)) + C\zeta\rho - A\zeta\rho\varphi^2 &= B\kappa - \rho\zeta((\alpha + 1)B - C) \\ &\geq -\zeta\rho((\alpha + 1)^2\zeta^2(1 - \rho^2) + \kappa^2) > 0 \end{aligned} \quad (11)$$

Squaring both sides of (11) and knowing that (12) is true, we have (13).

$$\begin{aligned} 2A(\kappa - \zeta\rho(\alpha + 1)) + B\zeta\rho &= \zeta^2(2\kappa - \zeta\rho) \geq 0, \\ B(\kappa - \zeta\rho(\alpha + 1)) + 2C\zeta\rho &= \zeta^2(\kappa(2\alpha + 1) - \zeta\rho(\alpha + 1)) \geq 0. \end{aligned} \quad (12)$$

$$\begin{aligned} -\zeta\rho\varphi^2 B(2A(\kappa - \zeta\rho(\alpha + 1)) + B\zeta\rho) \\ + B(\kappa - \zeta\rho(\alpha + 1))(B(\kappa - \zeta\rho(\alpha + 1)) + 2C\zeta\rho) \geq 0. \end{aligned} \quad (13)$$

Therefore, inequality (7) is true and so like in CASE 1,

$$\operatorname{Re}\left(\frac{\kappa - \rho\zeta(\alpha + 1) - \rho\zeta\varphi i}{-\bar{d}(\varphi)}\right) \geq 0 \quad \text{and hence } \bar{d}^*(\varphi) \text{ will never cross the negative}$$

real axis.

CASE 3:  $\rho > 0$  and  $(\kappa - \rho\zeta(\alpha + 1)) \geq 0$ .

Similar to CASE 2, notice that  $\operatorname{Re}(\bar{d}^*(\varphi)) < 0$  and  $\operatorname{Im}(\bar{d}^*(\varphi)) > 0$  holds and since

$(\kappa - \rho\zeta(\alpha + 1)) \geq 0$ , it implies that  $\zeta^2(2\alpha + 1) + 2\zeta\rho(\kappa - \zeta\rho(\alpha + 1)) \geq 0$ . Hence  $\bar{d}^*(\varphi)$  will never cross the negative real axis since

$$\operatorname{Re}\left(\frac{\kappa - \rho\zeta(\alpha + 1) - \rho\zeta\varphi i}{-\bar{d}(\varphi)}\right) \geq 0.$$

CASE 4:  $\rho > 0$ ,  $(\kappa - \rho\zeta(\alpha + 1)) < 0$  and  $\zeta^2(2\alpha + 1) + 2\rho\zeta(\kappa - \rho\zeta(\alpha + 1)) > 0$ .

$$\zeta^2(2\alpha + 1) + 2\rho\zeta(\kappa - \rho\zeta(\alpha + 1)) > 0 \Rightarrow \bar{d}(\varphi) = -\mu + iv \quad \text{where } \mu, v > 0 \quad \forall \varphi \in \mathbb{R}.$$

To show that  $\bar{d}^*(\varphi)$  cannot be in the second quadrant, let

$$\bar{d}^*(\varphi) = (\kappa - \rho(\alpha + 1)) \frac{1 - e^{\bar{d}(\varphi)t}}{-\bar{d}(\varphi)} - \zeta\rho\varphi i \frac{1 - e^{\bar{d}(\varphi)t}}{-\bar{d}(\varphi)} + 1 + e^{\bar{d}(\varphi)t}. \quad (14)$$

Observe that  $\arg\left(\frac{1 - e^{\bar{d}(\varphi)t}}{-\bar{d}(\varphi)}\right) = \tan^{-1}\left(\frac{\mu}{v}\right) - \tan^{-1}\left(\frac{\sin vt}{e^{\mu t} - \cos vt}\right) \leq \pi$ . So,

$$0 \leq \arg\left(\frac{1 - e^{\bar{d}(\varphi)t}}{-\bar{d}(\varphi)}\right) \leq \pi.$$

If  $\arg\left(\frac{1-e^{\bar{d}(\varphi)t}}{-\bar{d}(\varphi)}\right) \geq \frac{\pi}{2}$ , then  $\operatorname{Re}\left((\kappa-\zeta\rho(\alpha+1)-\zeta\rho\varphi i)\frac{1+e^{\bar{d}(\varphi)t}}{-\bar{d}(\varphi)}\right) \geq 0$  and so the

real part of  $\bar{d}^*(\varphi)$  is nonnegative since  $\operatorname{Re}(1-e^{\bar{d}(\varphi)t}) \geq 0$ . Hence  $\bar{d}^*(\varphi)$  cannot

be in the second quadrant. However, if  $\arg\left(\frac{1-e^{\bar{d}(\varphi)t}}{-\bar{d}(\varphi)}\right) < \frac{\pi}{2}$ , then

$-\rho\zeta\varphi i\left(\frac{1-e^{\bar{d}(\varphi)t}}{-\bar{d}(\varphi)}\right)$  is in the fourth quadrant and hence it is sufficient to confirm

that  $(\kappa-\zeta\rho(\alpha+1))\frac{1-e^{\bar{d}(\varphi)t}}{-\bar{d}(\varphi)}+e^{\bar{d}(\varphi)t}+1$  cannot be in the second quadrant. Let

$\kappa-\zeta\rho(\alpha+1)=-C < 0$ , then

$$\begin{aligned} -C\frac{1-e^{\bar{d}(\varphi)t}}{-\bar{d}(\varphi)}+e^{\bar{d}(\varphi)t}+1 &= -C\frac{1-e^{-\mu t}\cos vt-ie^{-\mu t}\sin vt}{\mu-iv}+e^{-\mu t}\cos vt+ie^{-\mu t}\sin vt+1 \\ &= \frac{(\mu^2+v^2)(e^{\mu t}+\cos vt)-C(\mu e^{\mu t}-\mu\cos vt+v\sin vt)}{e^{\mu t}(\mu^2+v^2)} \\ &\quad +i\frac{(\mu^2+v^2)\sin vt-C(v e^{\mu t}-v\cos vt-\mu\sin vt)}{e^{\mu t}(\mu^2+v^2)}. \end{aligned} \tag{15}$$

Thus,  $\operatorname{Im}(\bar{d}^*(\varphi)) > 0 \Rightarrow (\mu^2+v^2)\sin vt > C(v e^{\mu t}-v\cos vt-\mu\sin vt)$  and since

$C(v e^{\mu t}-v\cos vt-\mu\sin vt) > 0$ , it follows that  $\sin vt$  has to be positive and so

$$(\mu^2+v^2) > \frac{C(v e^{\mu t}-v\cos vt-\mu\sin vt)}{\sin vt}. \text{ Thus,}$$

$$\begin{aligned} \operatorname{sgn}(\operatorname{Re}(\bar{d}^*(\varphi))) &= \operatorname{sgn}((\mu^2+v^2)(e^{\mu t}+\cos vt)-C(\mu e^{\mu t}-\mu\cos vt+v\sin vt)) \\ &\geq \operatorname{sgn}\left(\frac{C(v e^{\mu t}-v\cos vt-\mu\sin vt)}{\sin vt}(e^{\mu t}+\cos vt)-C(\mu e^{\mu t}-\mu\cos vt+v\sin vt)\right) \\ &= \operatorname{sgn}(v e^{2\mu t}-\mu e^{\mu t}\sin vt-v) \geq \operatorname{sgn}(v(e^{2\mu t}-2\mu t e^{\mu t}-1)) = 1. \end{aligned}$$

Therefore, if  $\operatorname{Im}(\bar{d}^*(\varphi)) > 0$ , then  $\operatorname{Re}(\bar{d}^*(\varphi)) > 0$  and so  $\bar{d}^*(\varphi)$  cannot be in the second quadrant.

CASE 5:  $\rho > 0$ ,  $(\kappa-\rho\zeta(\alpha+1)) < 0$  and  $\zeta^2(2\alpha+1)+2\rho\zeta(\kappa-\rho\zeta(\alpha+1)) \leq 0$ .

Consider  $\bar{d}(\varphi) = -\mu - i\nu$  where  $\mu, \nu > 0 \quad \forall \varphi \in \mathbb{R}$ , then if  $\zeta^2(2\alpha + 1) + 2\rho\zeta(\kappa - \rho\zeta(\alpha + 1)) < 0$ , we have  $(\kappa - \rho\zeta(\alpha + 1))^2 - \zeta^2(\alpha + 1)\alpha > 0$  and so  $\mu > \nu$ . Also

$$\begin{aligned} \text{Im}(\bar{d}^*(\varphi)) &= \text{Im}\left(1 + e^{\bar{d}(\varphi)} + (1 - e^{\bar{d}(\varphi)}) \frac{\kappa - \rho\zeta(\alpha + 1) - \rho\zeta\varphi i}{-\bar{d}(\varphi)}\right) \\ &= \frac{-(\mu^2 + \nu^2 + \mu\omega + \rho\zeta\nu\varphi)\sin\nu t - (\mu\rho\zeta\varphi - \omega\nu)(e^{\mu t} - \cos\nu t)}{(\mu^2 + \nu^2)e^{\mu t}}, \end{aligned} \quad (16)$$

where  $\omega = \rho\zeta(\alpha + 1) - \kappa > 0$ . To show that our expression (16) is non-positive, we already know that the denominator  $(\mu^2 + \nu^2)e^{\mu t} > 0$ . From the numerator, we notice that

$$\begin{aligned} (\mu\omega + \rho\zeta\nu\varphi)(-\sin\nu t) - \mu t(\mu\rho\zeta\varphi - \nu\omega) &\leq \nu t(\mu\omega + \rho\zeta\nu\varphi) - \mu t(\mu\rho\zeta\varphi - \nu\omega) \\ &= t(\mu\nu\omega + \rho\zeta\nu^2\varphi - \rho\zeta\mu^2\varphi + \mu\nu\omega) \\ &= t(\rho\zeta(\nu^2 - \mu^2)\varphi + 2\mu\nu\omega). \end{aligned} \quad (17)$$

So, setting  $\tilde{A} = \zeta^2(1 - \rho^2) > 0$ ,  $\tilde{B} = 2\rho\zeta(\alpha + 1)\rho\zeta - \kappa - \zeta^2(2\alpha + 1) > 0$  and  $\tilde{C} = (\rho\zeta(\alpha + 1) - \kappa)^2 - \zeta^2(\alpha + 1)\alpha > 0$ , we can rewrite  $\bar{d}(\varphi)$  as

$$\bar{d}(\varphi) = -\left(\sqrt{\frac{\sqrt{(\tilde{A}\varphi^2 + \tilde{C})^2 + \tilde{B}^2\varphi^2} + (\tilde{C} - \tilde{A}\varphi^2)}{2}} + i\sqrt{\frac{\sqrt{(\tilde{A}\varphi^2 + \tilde{C})^2 + \tilde{B}^2\varphi^2} - (\tilde{C} + \tilde{A}\varphi^2)}{2}}\right).$$

Using the new notation,  $t(\rho\zeta(\nu^2 - \mu^2)\varphi + 2\mu\nu\omega) = t\varphi(\tilde{B}\omega - \rho\zeta(\tilde{A}\varphi^2 + \tilde{C}))$ . Since  $\tilde{B} - \rho\zeta\tilde{C} < 0$ , it follows that

$$\begin{aligned} \tilde{B}\omega - \rho\zeta\tilde{C} &= \rho\zeta(\rho\zeta(\alpha + 1) - \kappa)^2 + \rho\zeta^3(\alpha^2 + \alpha) - \zeta^2(2\alpha + 1)(\rho\zeta(\alpha + 1) - \kappa) \\ &= \zeta^2\alpha\kappa(1 - \rho^2) - \rho\zeta\kappa(\rho\zeta - \kappa) - \zeta^2(\alpha + 1)(1 - \rho^2)(\rho\zeta(\alpha + 1) - \kappa) \\ &= -\zeta^2\alpha(1 - \rho^2)(\rho\zeta(\alpha + 1) - 2\kappa) - \rho\zeta\kappa(\rho\zeta - \kappa) - \zeta^2(1 - \rho^2)(\rho\zeta(\alpha + 1) - \kappa). \end{aligned}$$

Since  $\tilde{B} > 0 \Rightarrow \rho\zeta - 2\kappa > 0$  and so (17) is non-positive. Thus, to show that (16) is non-positive it suffices to prove that  $-(\mu^2 + \nu^2) \sin vt - (e^{\mu t} - \mu t - \cos vt)(\mu\rho\zeta\varphi - \omega\nu) \leq 0$ . This is true when  $vt \leq \pi$  and so as  $\mu \geq \nu$  we can assume that  $\mu t > \pi$  and verify that  $e^{\mu t} - \mu t - \cos vt > 2\mu t$ . Thus,

$$\begin{aligned} & -(\mu^2 + \nu^2) \sin vt - (e^{\mu t} - \mu t - \cos vt)(\mu\rho\zeta\varphi - \omega\nu) \\ & \leq vt(\mu^2 + \nu^2) - 2\frac{\mu}{\tilde{B}}\mu t(\rho\zeta\sqrt{(\tilde{A}\varphi^2 + \tilde{C})^2 + \tilde{B}^2\varphi^2} + \rho\zeta(\tilde{A}\varphi^2 + \tilde{C}) - \tilde{B}\omega) \\ & \leq \frac{vt}{\tilde{B}}(\tilde{B} - 2\rho\zeta\mu)\sqrt{(\tilde{A}\varphi^2 + \tilde{C})^2 + \tilde{B}^2\varphi^2}. \end{aligned}$$

Since  $\mu^2 = \tilde{C} \Rightarrow 4\rho^2\zeta^2\tilde{C} \geq \tilde{B}^2 \Rightarrow 4\rho^2\zeta^2\mu^2 \geq \tilde{B}^2 \Leftrightarrow 2\rho\zeta\mu \geq \tilde{B}$ . Also, using the fact that  $\rho\zeta(\rho\zeta(\alpha+1) - \kappa) > \frac{\zeta^2(2\alpha+1)}{2}$ , we have

$$\begin{aligned} 4\rho^2\zeta^2\tilde{C} - \tilde{B} & \geq \frac{4\zeta^2(2\alpha+1)}{2}\zeta^2(2\alpha+1) - 4\rho^2\zeta^2(\alpha^2 + \alpha) - \zeta^4(2\alpha+1)^2 \\ & = \zeta^4(2\alpha+1)^2 - 4\rho^2\zeta^2(\alpha^2 + \alpha) \\ & = 4\zeta^4(\alpha^2 + \alpha)(1 - \rho^2) + \zeta^4 > 0. \end{aligned}$$

Hence, the proof is complete.

## 5 Conclusion

Detailed investigation on the sensibility of Heston model parameters for options pricing using numerical approach is given. The analytic characteristic function of the model where there existed a potential branch-cut is examined for discontinuity and instability. Condition under which the characteristic function guaranteed stability for full dimensional and unrestricted parameter space is established.

## References

- [1] Black, F. and Scholes M., The Valuation of Options and Corporate Liabilities, *Journal of Political Economy*, **1**(81), (1973), 637 - 654.
- [2] Cont, Rama, Empirical Properties of Asset Returns: Stylized Facts and Statistical Issues, *Quantitative Finance*, **1**, (2001), 223-236.
- [3] Bakshi, Gurdip, Charles Cao and Zhiwu Chen, Empirical Performance of Alternative Option Pricing Models, *The Journal of Finance*, **52**, (1997), 2003-2049.
- [4] Bates, David S., Jumps and Stochastic Volatility: Exchange Rate Processes Implicit in Deutsche Mark Options, *The Review of Financial Studies*, **9**, (1996), 69-107.
- [5] Bates, David S., Post-87 Crash Fears in S&P 500 Futures Options, *Journal of Econometrics*, **94**, (2000), 181-238.
- [6] Christoffersen, Peter, Steven Heston and Kris Jacobs, The Shape and Term Structure of the Index Option Smirk: Why Multifactor Stochastic Volatility Models Work so Well, *Working Paper*, McGill University, 2009.
- [7] Hull, J., and White, A. The Pricing of Options on Assets with Stochastic Volatilities. *Journal of Finance*, **42**, (1987), 281-300.
- [8] Mikhailov, Sergei and Ulrich Ngel, 2003, Heston's Stochastic Volatility Model Implementation, Calibration and Some Extensions, *Wilmott Magazine*, **4**, (2003), 74-79.
- [9] Stein, E. M., & Stein, J. C., Stock price distributions with stochastic volatility: An analytic approach, *Review of Financial Studies*, (1991), 727-752.
- [10] Scott, E., & Tucker, A. L., Predicting currency return volatility, *Journal of Banking and Finance*, **13**(6), (1989), 839-851.
- [11] Heston, S. A closed-form solution for options with stochastic volatility with applications to bond and currency options, *Review of Financial Studies*, **6**, (1993), 327-343.

- [12] Kahl, C. and Jackel, P., 'Not-so-complex logarithms in the heston model', *WILMOTT magazine*, (2005), 94-103.
- [13] Kruse, S. and Nogel, U., 'On the pricing of forward starting options in heston's model on stochastic volatility', *Finance Stochast*, **9**(2), (2005), 233-250.
- [14] Lord, Roger and Kahl, Christian, Why the Rotation Count Algorithm Works, *Tinbergen Institute Discussion Paper*, **2006-065/2**, (2006), available at SSRN:  
<http://ssrn.com/abstract=921335> or <http://dx.doi.org/10.2139/ssrn.921335>.
- [15] Mikhailov, S. and Nogel, U., 'Heston's stochastic volatility model implementation, calibration and some extensions', *WILMOTT magazine*, **7**, (2003).
- [16] Lucic, V. Forward start options in stochastic volatility models, *Wilmott Magazine*, September Issue, 2003.
- [17] Gatheral J., *The Volatility Surface*, A Practitioner's Guide, Wiley, 2006.